

Differentiation of HIV-associated lymphoma from HIV-associated reactive adenopathy using quantitative FDG PET and symmetry

Joyce C. Mhlanga · Daniel Durand · Hua-Ling Tsai ·
Christine M. Durand · Jeffrey P. Leal · Hao Wang ·
Richard Moore · Richard L. Wahl

Received: 15 August 2013 / Accepted: 10 December 2013 / Published online: 28 January 2014
© Springer-Verlag Berlin Heidelberg 2014

Abstract

Purpose To determine the diagnostic accuracy of a semiautomated ^{18}F -FDG PET/CT measurement of total lesion glycolysis (TLG), maximum and peak standardized uptake value at lean body mass (SUL-Max and SUL-Peak), qualitative estimates of left/right nodal symmetry and FDG uptake for differentiating lymphoma from reactive adenopathy in HIV-infected patients.

Methods We retrospectively analyzed 41 whole-body ^{18}F -FDG PET/CT studies performed in HIV-infected patients for clinical reasons. The study received institutional review board approval. Of the 41 patients, 19 had biopsy-proven untreated lymphoma, and 22 with reactive adenopathy without malignancy on follow-up were used as controls. Nodal and extranodal visual qualitative metabolic scores, SUL-Max, SUL-Peak, CT nodal size, and PERCIST 1.0 threshold-based TLG and metabolic tumor volume (MTV) were determined. The qualitative intensity of nodal involvement and

symmetry of uptake were compared using receiver operator curve (ROC) analysis. HIV plasma viral RNA measurements were also obtained.

Results All of the quantitative PET metrics performed well in differentiating lymphoma from reactive adenopathy and performed better than qualitative visual intensity scores. The areas under the ROC curves (AUC) were significantly higher for TLG=0.96, single SUL-Peak=0.96, single SUL-Max=0.97, and MTV=0.96, compared to 0.67 for CT nodal size ($p<0.001$). These PET metrics performed best in separating the two populations in aviremic patients, with AUCs of 1 (AUC 0.91 for CT nodal size). TLG, MTV, SUL-Peak and SUL-Max were more reliable markers among viremic individuals, with AUCs between 0.84 and 0.93, compared to other metrics. PET metrics were significantly correlated with plasma viral load in HIV-reactive adenopathy controls. Asymmetrical FDG uptake had an accuracy of 90.4 % for differentiating lymphoma from reactive adenopathy in HIV-infected patients.

Conclusion Quantitative PET metabolic metrics as well as the qualitative assessment of symmetry of nodal uptake appear to be valuable tools for differentiating lymphoma from reactive adenopathy in HIV-infected patients using FDG PET. These parameters appear more robust in aviremic patients.

A related editorial commentary can be found at doi 10.1007/s00259-014-2701-2

J. C. Mhlanga · D. Durand · J. P. Leal · R. L. Wahl (✉)
Division of Nuclear Medicine, The Russell H. Morgan Department
of Radiology and Radiological Sciences, Johns Hopkins University
School of Medicine, Baltimore, MD, USA
e-mail: rwahl@jhmi.edu

H.-. Tsai · H. Wang
Department of Oncology Biostatistics Division, Johns Hopkins
University School of Medicine, Baltimore, MD, USA

C. M. Durand · R. Moore
Maryland Infectious Diseases Department, Johns Hopkins
University School of Medicine, Baltimore, MD, USA

R. L. Wahl
Department of Oncology, Johns Hopkins University School of
Medicine, Baltimore, MD, USA

Keywords PET/CT · HIV · Lymphoma · Lymphadenopathy · TLG

Introduction

HIV infection causes acquired immunodeficiency syndrome (AIDS) via defective cell-mediated immunity secondary to progressive depletion of CD4^+ T lymphocytes, immune dysregulation and sustained viral production [1]. Several

malignancies are increased in patients with HIV infection, including non-Hodgkin lymphoma, which is an AIDS-defining cancer as well as Hodgkin lymphoma [2]. There has been a rising incidence of AIDS-related cancers, possibly because antiretroviral therapy (ART) prolongs patient survival and causes dysfunctional cell-mediated immunity [3, 4].

^{18}F -FDG PET/CT can demonstrate abnormal foci of increased FDG accumulation in HIV-infected individuals with suspected malignancy or fever of unknown origin (FUO) by localizing to malignant or inflammatory cells such as neutrophils and macrophages [5–9]. Activated lymphocytes exhibit increased glucose utilization and HIV-infected individuals have a greater accumulation of FDG in their lymph nodes than patients without HIV infection [6, 10]. The amount of HIV RNA in the peripheral blood is correlated with the amount of viral replication in lymph nodes [11]. ^{18}F -FDG PET/CT is also valuable in the management of HIV-infected patients with lymphoma [6, 12]. In lymphadenopathy due to lymphoma the nodes are often enlarged with intense FDG uptake in comparison to those in reactive lymphadenopathy without malignancy [13], although these entities can overlap in appearance. There are no rigorously defined quantitative PET methods to differentiate these entities.

Differentiating lymphoma from reactive adenopathy in HIV-infected patients with ^{18}F -FDG PET/CT can be challenging, especially in the setting of high plasma HIV RNA in which FDG-avid nodes commonly occur. In this retrospective study we investigated the diagnostic accuracy of quantitative FDG PET/CT metrics and compared their performance with those of qualitative PET metrics and CT. Our overall goal was to better differentiate between nonmalignant reactive adenopathy and lymphoma in HIV-infected patients.

Material and methods

Study population

The study was HIPAA-compliant and received institutional review board approval with a waiver of written informed consent for a retrospective study. Patients who had undergone a whole-body ^{18}F -FDG PET/CT study between 2006 and 2010 were identified from the Radiology Information Systems and the local HIV clinic database. We identified 19 patients (47 ± 11.7 years) with untreated biopsy-proven HIV-associated lymphoma (16 large B-cell lymphoma, 3 Hodgkin lymphoma) who had undergone PET/CT prior to chemotherapy (7 in whom the primary diagnosis of lymphoma was made following PET/CT without a significant delay between PET/CT and subsequent biopsy). We also identified a suitable control group of 22 patients (50 ± 9.7 years) with HIV without any known underlying malignancy who had undergone PET/CT with identical protocols over the same period comprising

12 patients for evaluation of solitary pulmonary nodules (SPN) and 10 patients with FUO (Table 1). Prescan plasma viral load (single determinant), CD4^+ count, pathology, culture and results of follow-up imaging were obtained. None of the SPN group had malignancy on follow-up.

^{18}F -FDG PET/CT study and image analysis

^{18}F -FDG PET/CT studies were performed using either a Discovery VCT (RX) system in 3-D or a Discovery LS PET/CT scanner in 2-D (both GE Healthcare, Waukesha, WI) using standard protocols with a 60-min target uptake period [14, 15]. CT scans were used for attenuation correction of the PET emission data and lesion size measurements.

All 41 PET/CT studies were retrospectively analyzed qualitatively and semiquantitatively in a blinded manner by a single independent investigator with CT and PET training, with verification by a second trained reader. The pattern and intensity of FDG accumulation were also assessed in bilateral

Table 1 Characteristics of HIV-infected patients

Characteristic	Lymphoma (N=19)	Reactive adenopathy (N=22)	<i>p</i> value ^a
Age (years), mean \pm SD	47 \pm 11.7	50 \pm 9.7	0.424
Sex, <i>n</i>			
Male	13	14	1.00
Female	6	8	
Lymphoma subtypes, <i>n</i>			
DLCL	16	–	–
Hodgkin	3	–	–
PET/CT indications, <i>n</i>			
Lymphoma diagnosis and staging	19	0	
Fever of unknown origin	0	10	
Pulmonary nodules	0	12	
Combination antiretroviral therapy			
Yes	18	13	0.011
Antiretroviral therapy-naive	1	9	
Plasma HIV RNA (copies/mL, log ₁₀ scale)			
Mean \pm SD	2.22 \pm 2.17	2.76 \pm 2.19	0.41
Median	2.07	3.24	
CD4 count (cells/ μ l)			
Mean \pm SD	356 \pm 344	428 \pm 359	0.31
Viremia			
Aviremia	10	10	0.76
Viremia	9	12	
Time from PET to last follow-up (years), median	3.2	4.1	0.39
Uptake time (min), mean \pm SD	62.6 \pm 9.5	62.0 \pm 10.6	0.79
Dose (MBq), mean \pm SD	614.2 \pm 185	588.3 \pm 187	0.68

^a*p* values were based on Fisher's exact test for categorical predictors, or Wilcoxon's test for continuous predictors

cervical, axillary, mediastinal, hilar, periaortic, iliac and inguinal nodal regions, and in extranodal sites of lymphoma. Qualitative visual glycolytic scores were determined for PET/CT for each nodal region using a five-point scale from low to high uptake (0–4): 0 no nodal activity, 1 activity < descending aortic blood pool, 2 activity similar to blood pool, 3 activity \leq liver but > blood pool, 4 activity > liver uptake. The highest single qualitative visual nodal score in the whole body and the summed qualitative score of all the nodal groups were determined for each patient. The utility of a visual symmetry score for differentiating lymphoma from reactive adenopathy in HIV-infected patients was also evaluated. A simple binary score was used to assess the symmetry of nodal FDG uptake (0 asymmetry, 1 symmetry) based on the rotating maximum intensity projection (MIP) images. FDG uptake in patients without apparent adenopathy but extranodal sites of lymphoma was also scored as asymmetrical.

The maximum standardized uptake value at lean body mass (SUL-Max) was recorded manually for the hottest nodes in each of the nodal regions using an AW workstation (GE Healthcare) and a summed nodal (and/or extranodal) SUL-Max score was determined for each patient. The single hottest nodal SUL-Max value in the whole body was also recorded. The summed CT nodal size from all the described nodal regions on the noncontrast low-dose CT component was calculated measuring the maximum short axis diameter of the node. The highest SUL-Max score was also determined for the nasopharyngeal region as described by Liu [16]. A semiautomated software tool (Auto-PERCIST™: A PET Image Volume Viewer with Integrated PERCIST-based Computer Assisted Analysis [software]. Baltimore, MD: The Johns Hopkins University; 2013) was used to obtain the total lesion glycolysis (TLG), metabolic tumor volume (MTV), SUL-Max and SUL-Peak of the single hottest lesion, and sum SUL-Peak of nodes and extranodal lesions as defined in PERCIST 1.0 [17]. Disease was defined as abnormal metabolic uptake above a set baseline threshold of $1.5 \times$ liver mean + 2 standard deviations (SD) [17]. Liver background was determined according to PERCIST 1.0. Areas of normal physiological activity such as the heart, brain, kidneys and bladder were manually excluded from the analysis.

Subgroup analysis of the patients with FUO against those with lymphoma was also performed to determine whether FDG PET performs similarly in the febrile and the nonfebrile HIV population.

Statistical analysis

The continuous variables in HIV-infected patients with lymphoma and those with reactive adenopathy were compared using the Wilcoxon test. Correlations between viral load and the sum SUL-Max, sum SUL-Peak, TLG, MTV, and CT nodal size were determined with Spearman's correlation

coefficients (r). Univariate analysis was performed for each imaging marker using logistic regression to assess its performance in differentiating lymphoma from reactive adenopathy. Multivariate logistic regression analysis was used to identify a subset of relevant PET parameters that could potentially be used in routine practice for differentiating lymphoma and reactive adenopathy in HIV-infected patients by applying a stepwise backward elimination based on the Akaike information criterion (AIC). Receiver operating characteristic (ROC) analysis using univariate logistic models was used to quantify the discriminatory ability of TLG, SUL-Max, SUL-Peak, MTV and CT nodal size metrics for differentiating lymphoma from reactive adenopathy. The cut-off values and corresponding sensitivity, specificity, positive predictive value (PPV), and negative predictive value (NPV) were determined. DeLong's method was applied to compare the areas under the curve (AUCs) among the different metrics.

We further evaluated the performance of the quantitative metrics stratified by the presence of viremia. Our definition of viremia was based on a single prescan HIV plasma RNA measurement of >200 copies/mL as per the latest US Department of Health and Human Services guidelines [18, 19].

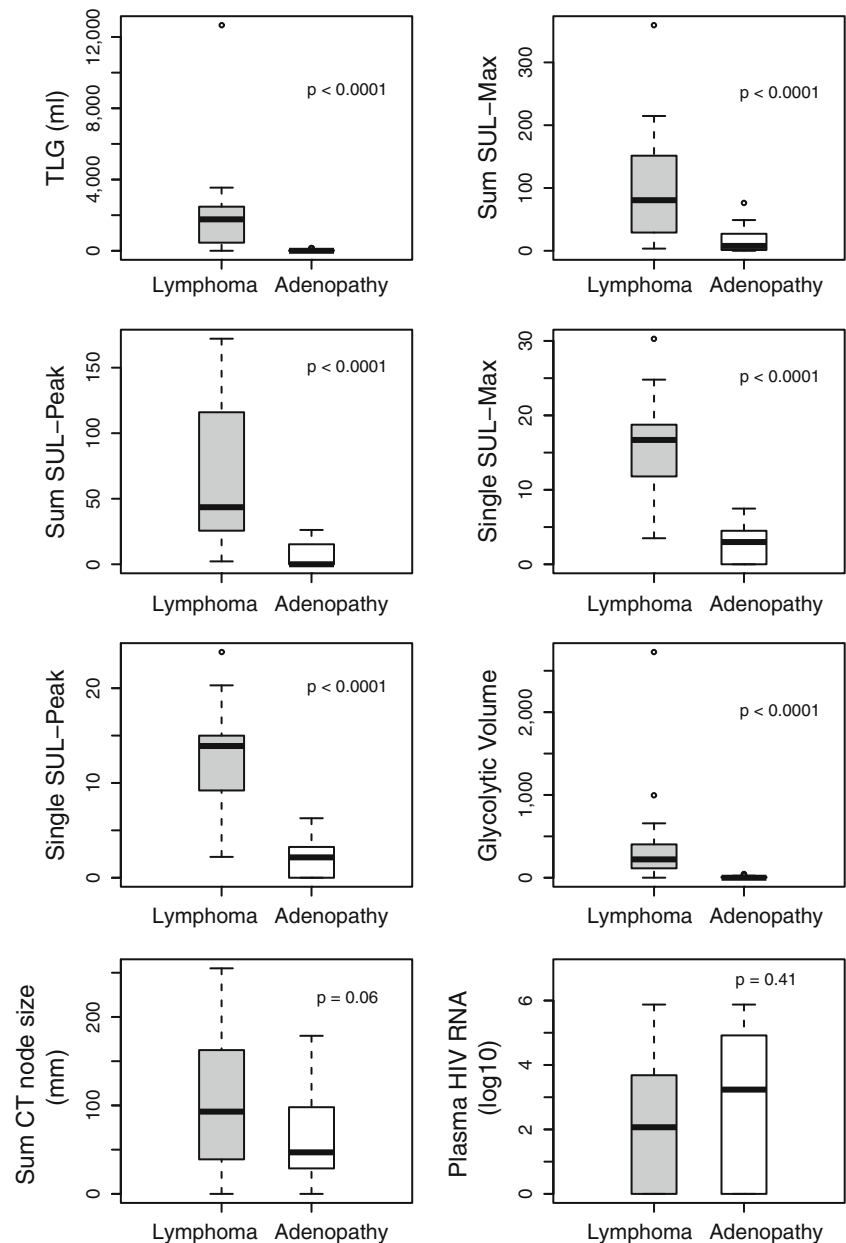
Kappa statistics were used to evaluate the interreader agreements for visual symmetry, and 95 % confidence intervals were calculated by assuming a normal distribution of the kappa coefficient with variance [20]. Univariate analysis was performed to assess the diagnostic performance of the symmetry score. Spearman's rank correlation was used to evaluate the association between the symmetry score and quantitative computer-aided detection analysis. All tests are two-sided and p values <0.05 were considered to indicate statistical significance. The statistical software R (version 2.14.1) was used for the analysis.

Results

The single hottest SUL-Max, summed nodal SUL-Max, semiautomated single hottest SUL-Peak, summed SUL-Peak, TLG and MTV were significantly higher in patients with lymphoma than in those with reactive adenopathy (Fig. 1, Table 2), and CT nodal size trended towards a difference ($p=0.06$). There was no significant difference in the viral load or CD4 counts between the lymphoma and the nonlymphoma groups ($p=0.41$ and 0.51 , respectively; Table 1).

Univariate logistic models for determining the accuracies of each described quantitative metabolic metric and CT nodal size for differentiating lymphoma from reactive adenopathy revealed AUCs of 0.97 for the single hottest SUL-Max, 0.905 for sum SUL-Max, 0.96 for the single hottest SUL-Peak, 0.94 for sum SUL-Peak, 0.964 for TLG, 0.96 for MTV, and 0.67 for CT nodal size (Fig. 2). The PET metrics performed significantly better

Fig. 1 Values of metabolic imaging markers in relation to lymphoma status in all patients. PET metrics and CT nodal size were significantly higher in HIV patients with lymphoma than in those with reactive adenopathy. The bottom and top of the box represent the 25 % and 75 % quartiles; the whiskers indicate the range of data when excluding outliers (defined as 1.5 times the interquartile range, i.e. difference between 75 % and 25 % quartiles)



than CT nodal size ($p < 0.001$). A TLG cut-off of 173 yielded a sensitivity of 89 % and specificity of 100 % for differentiating lymphoma from reactive adenopathy. A summed SUL-Peak cut-off of 23.8 yielded a sensitivity and specificity of 84 % and 95 %, whereas a summed SUL-Max cut-off of 28.4 yielded a sensitivity of 84 % and specificity of 82 % (Table 3). In the multivariate analysis the AUC for the single SUL-Max and sum CT nodal size parameters combined was 0.974. This was not significantly higher than the individual AUCs from the univariate analysis for the single SUL-Max, single SUL-Peak, TLG or MTV, and therefore did not provide significant improvement in the ability to differentiate lymphoma from reactive adenopathy in HIV-infected patients.

The differences in qualitative nodal visual intensity scores between HIV patients with lymphoma and those with reactive adenopathy were not statistically significant (Table 2).

Stratification of metabolic metrics by viremia (HIV plasma RNA > 200 copies/mL) revealed 21 aviremic patients, 10 with lymphoma and 11 without lymphoma. In the aviremic patients, sum SUL-Max, sum SUL-Peak, TLG, MTV, single hottest SUL-Max and SUL-Peak performed best with AUCs of 1, with CT nodal size having an AUC of 0.905. In viremic patients with plasma HIV RNA levels > 200 copies/mL, single SUL-Max and SUL-Peak of the hottest lesion and TLG performed best with AUCs of 0.93, 0.91 and 0.86, respectively; MTV (AUC 0.84), sum SUL-Peak (0.80), sum SUL-Max

Table 2 Qualitative and quantitative FDG PET/CT metrics (values are means \pm SD unless stated otherwise)

Metric	HIV-associated lymphoma (N=19)	HIV-associated reactive adenopathy (N=22)	P value ^a
Single SUL-Max	15.9 \pm 6.8	2.9 \pm 2.4	<0.0001
TLG			
Mean \pm SD	2,146.5 \pm 2,778.5	30.6 \pm 53.8	<0.0001
Median (range)	1,766 (1.97 – 12,660)	1.0 (1.0 – 153.3)	
Single SUL-Peak	12.6 \pm 5.7	2.0 \pm 2.0	<0.0001
Glycolytic volume/MTV	409.8 \pm 611.5	9.6 \pm 14.5	<0.0001
Sum SUL-Peak	69.3 \pm 54.5	7.2 \pm 9.1	<0.0001
Sum SUL-Max	104.3 \pm 88.9	16.3 \pm 20.2	<0.0001
Summed CT nodal size	104.5 \pm 73.5	61.8 \pm 48.5	0.06
Single nodal visual score ^b , reader 1			
Median (range)	4 (0 – 4)	4 (0 – 4)	0.24
Sum nodal visual score, reader 1			
Median (range)	24 (0 – 60)	11.5 (0 – 66)	0.41
Nasopharyngeal region SUL-Max	3.5 \pm 3.2	3.7 \pm 2.9	0.54

^a Wilcoxon test^b Qualitative visual intensity score

(0.74), and CT nodal size (AUC 0.463, $p=0.95$) performed less well (Fig. 3).

In the HIV control group, a positive correlation was found between viral load and the following variables: summed and single hottest nodal SUL-Max ($r=0.58$ and 0.56 , $p=0.005$ and

0.007 , respectively), sum and single hottest SUL-Peak ($r=0.68$ and 0.50 , $p=0.001$ and 0.02 , respectively), sum TLG ($r=0.59$, $p=0.004$), CT nodal size ($r=0.63$, $p=0.019$), and MTV ($r=0.63$, $p=0.002$). However, in the subgroup of HIV-infected patients with lymphoma, none of the imaging parameters showed a significant correlation with viral load (data not shown).

Visual qualitative analysis of the pattern of lymph node involvement using the MIP qualitative symmetry score (where 0 indicates asymmetry and 1 indicates symmetry) was performed (Table 4). Reader 1 scored 86.4 % of the patients without lymphoma as score 1, and 5.3 % of the patients with

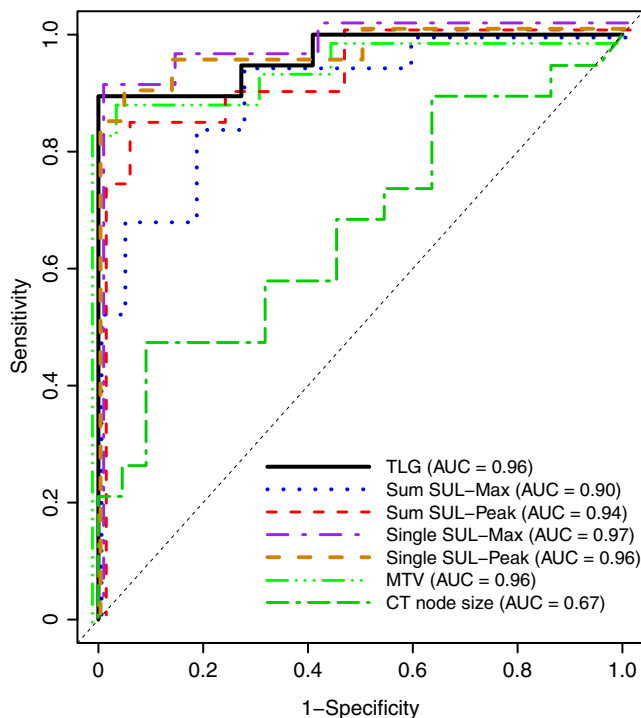


Fig. 2 ROC curves of the imaging markers in all patients. Sensitivity and specificity at each threshold value were computed on the basis that patients whose marker value was larger than the threshold were classified as having lymphoma. The AUC of CT nodal size is significantly smaller than those of the other markers ($p<0.05$). This indicates that FDG PET metrics are highly accurate in differentiating lymphoma from reactive adenopathy in HIV-infected patients

Table 3 FDG PET/CT metrics and cut-off points for predicting lymphoma in HIV-infected patients

Metric	Cut-off	Sensitivity (%)	Specificity (%)	PPV (%)	NPV (%)	AUC
Single SUL-Max	7.8	89	100	100	92	0.971
TLG	173	89	100	100	92	0.964
Single SUL-Peak	6.6	84	100	100	88	0.964
Glycolytic volume/MTV	53.8	84	100	100	88	0.957
Sum SUL-Peak	23.8	84	95	94	88	0.935
Sum SUL-Max	28.4	84	82	80	86	0.904
Summed CT nodal size	82.6	58	68	61	65	0.671
Single nodal visual score, reader 1	3.5	84	32	52	70	0.581
Sum nodal visual score, reader 1	23.5	53	64	56	61	0.576
Nasopharyngeal region SUL-Max	4.0	42	73	57	59	0.443 ^a

^a Negative class prediction

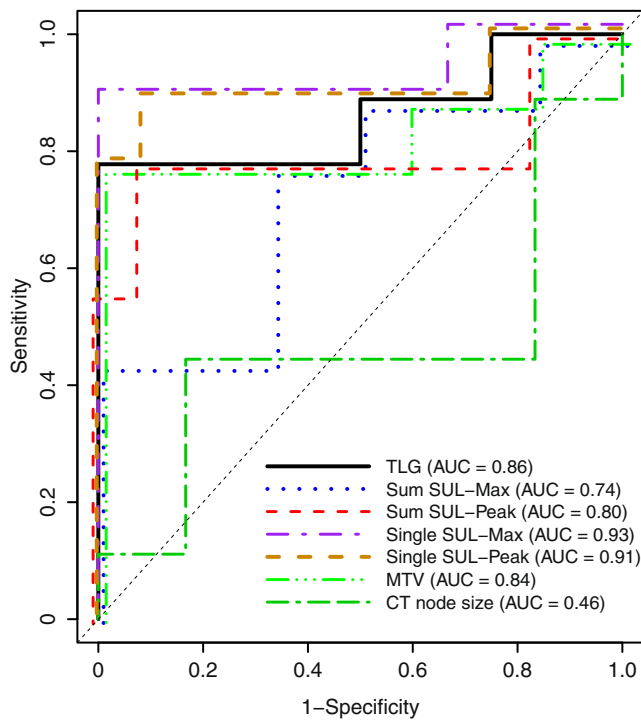


Fig. 3 ROC curves for viremic patients (plasma HIV RNA >200 copies/mL). PET metrics performed better than CT in differentiating lymphoma from reactive adenopathy, but less well than in aviremic patients (plasma HIV RNA <200 copies/mL) with AUCs of 1 for all the PET metrics and 0.91 for CT nodal size

lymphoma as score 1, giving a sensitivity of 94.7 %, a specificity of 86.4 %, a PPV of 85.7 %, and a NPV of 95 % for predicting lymphoma. Reader 2 scored 90.9 % of the patients without lymphoma as score 1, and 10.5 % of the patients with lymphoma as score 1, giving a sensitivity of 89.5 %, a specificity of 90.9 %, a PPV of 89.5 % and a NPV of 90.9 % for predicting lymphoma. The two readers had almost perfect agreement using the qualitative MIP symmetry score (kappa coefficient 0.90, 95 % CI 0.77 – 1.00) [20]. Overall, asymmetrical FDG uptake had an accuracy of 90.4 % for differentiating lymphoma from reactive adenopathy in HIV-infected patients for both readers.

HIV patients with lymphoma showed asymmetrical uptake, significantly higher PET metrics, as well as the presence of abdominal lymph node involvement and other extranodal

Table 4 MIP symmetry scores in relation to disease status for readers 1 and 2

HIV patient group	Reader 1		Reader 2	
	Symmetry score 0	Symmetry score 1	Symmetry score 0	Symmetry score 1
Reactive adenopathy	3	19	2	20
Lymphoma	18	1	17	2

A score of 0 indicates lack of symmetry, and a score of 1 indicates symmetry

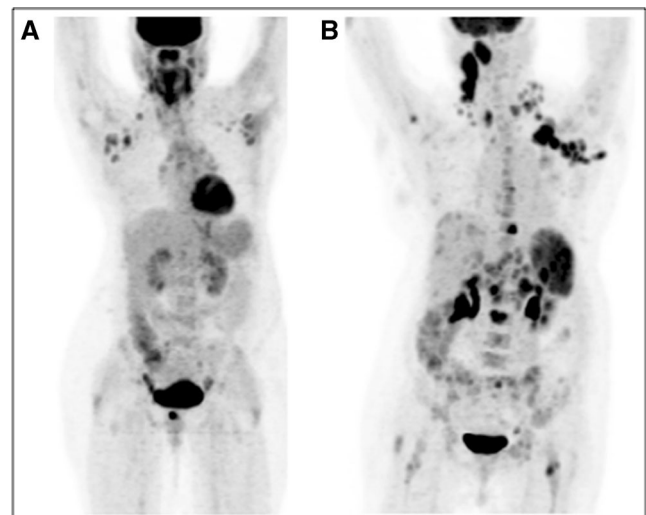


Fig. 4 Whole-body FDG PET/CT MIP images demonstrating symmetrical and asymmetrical uptake. **a** Relatively symmetrical bilateral cervical, axillary and mediastinal adenopathy in a patient with reactive adenopathy. **b** Asymmetrical FDG uptake greater in the right cervical, left axillary and retroperitoneal nodes, with splenic and marrow involvement of the spine and left femur in a patient with biopsy-proven HIV-associated lymphoma. Assessment of nodal symmetry aids in differentiating lymphoma from reactive adenopathy in patients with HIV infection

sites of disease. This extensive disease was not seen in HIV patients with reactive adenopathy (Figs. 4 and 5). The mean splenic metabolic uptake was higher in patients with lymphoma than in those with reactive adenopathy (SUL-Max 5.25 ± 6.17 vs. 2.41 ± 0.81 , $p=0.04$).

The separate analysis comparing HIV patients without lymphoma (10 patients) and those with lymphoma showed no significant difference in CT nodal size ($p=0.36$). ROC analysis for differentiating lymphoma and reactive adenopathy revealed AUCs of 0.95 for the single hottest SUL-Max, 0.88 for sum SUL-Max, 0.94 for the single hottest SUL-Peak, 0.91 for sum SUL-Peak, 0.95 for TLG, 0.94 for MTV, and 0.61 for CT nodal size. Again, all the PET metrics performed significantly better than CT nodal size ($p \leq 0.001$).

There was no significant difference in the mean SUL-Max scores of the nasopharyngeal region between patients with lymphoma the those with reactive adenopathy ($p=0.54$, Table 2). There was no correlation with viral load and the SUL-Max of nasopharyngeal lesions in either patient group ($r=0.011$, $p=0.96$, and $r=0.04$, $p=0.86$, respectively). When stratified by viremia status, FDG uptake in the nasopharyngeal region differentiated poorly between lymphoma and reactive adenopathy, with an AUC of 0.46 in aviremic patients and 0.41 in viremic patients.

Discussion

Differentiating reactive adenopathy from malignant nodes due to lymphoma in HIV-infected patients is challenging as both

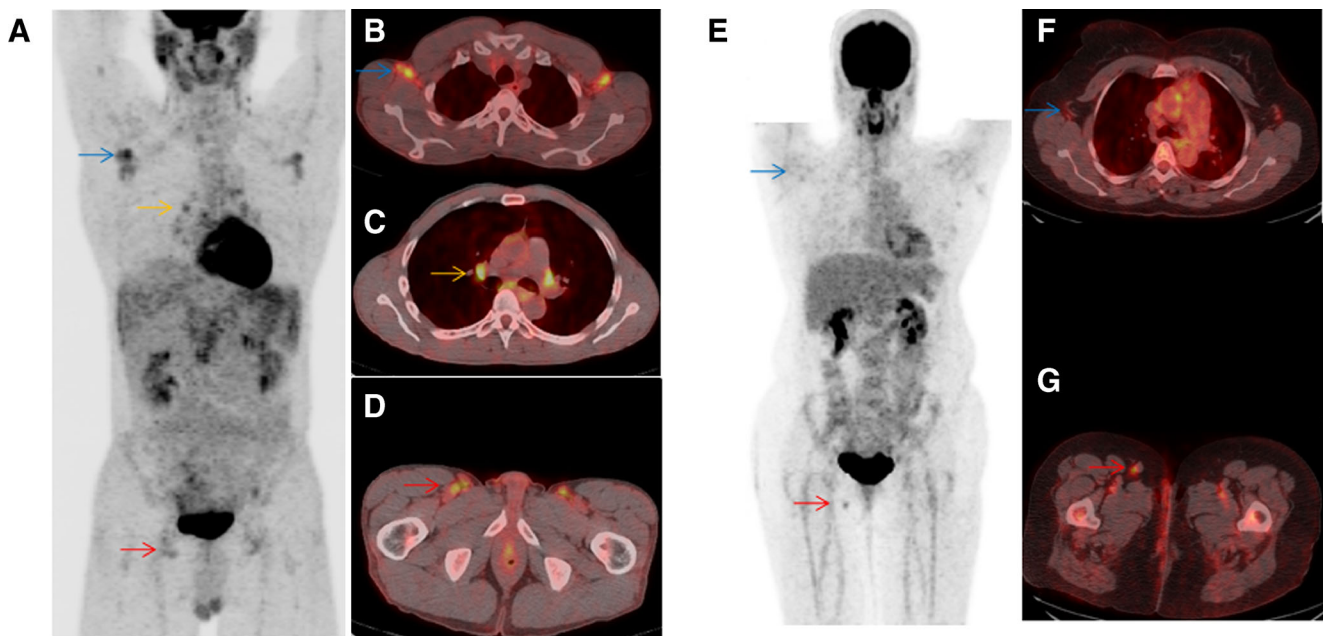


Fig. 5 Whole-body FDG PET/CT images in HIV-infected patients, one (a–d) with reactive adenopathy, a high level of viremia and increased nodal metabolic activity and the other (e–g) with a low level of viremia and low nodal metabolic activity. a–d The MIP image (a) and the fused axial PET/CT images (b–d) show symmetrical bilateral axillary (blue arrows), mediastinal (yellow arrows) and inguinal adenopathy (red arrows). The sum

SUL-Max was 27.1, and the plasma HIV RNA was 98,203 copies/mL. e–g The MIP image (e) and the fused axial PET/CT images (f, g) show mildly FDG avid bilateral axillary (blue arrows) and inguinal (red arrows) nodes. The sum SUL-Max was 9.6, and plasma HIV RNA was 64 copies/mL. The level of viremia correlated with the intensity of nodal metabolic uptake in HIV-infected patients with reactive adenopathy

conditions can be associated with increased FDG uptake. In this retrospective study we evaluated several quantitative and qualitative methods which could aid in the differentiation of lymphoma and reactive adenopathy in HIV-infected patients. Our major findings were that quantitative metabolic PET metrics performed better than CT nodal size in differentiating lymphoma from reactive adenopathy. Qualitative assessments of symmetry of uptake were also more robust than CT nodal size assessments. Nodal and extranodal qualitative and quantitative PET metrics were higher and CT nodal size larger in HIV-infected patients with lymphoma than in those with reactive adenopathy, but CT nodal size was similar between the patient groups. The MIP symmetry score showed an asymmetrical pattern of FDG uptake in lymphoma in contrast to the pattern in reactive adenopathy. SUL increased with increasing viral load in HIV-infected patients with reactive adenopathy, but quantitative FDG PET metrics were high in HIV-infected patients with lymphoma irrespective of the viral load. Our data are consistent with previous studies that have shown increased maximum standardized uptake value (SUV-Max) in HIV-infected patients with lymphoma [21, 22]. We evaluated the performance of quantitative semiautomated PET/CT data by including SUL-Peak and the volumetric TLG and MTV metrics.

All the quantitative PET metrics performed well in differentiating lymphoma from reactive adenopathy in HIV-infected patients particularly in aviremic patients, and were

correlated with the serum viral load in patients with reactive adenopathy. Multivariate analysis did not show a significant improvement in the ability of the combined quantitative PET metrics to differentiate lymphoma from reactive adenopathy in HIV-infected patients when compared with each individual PET metric. Thus each of the individual quantitative PET metrics appears to perform well enough to be used alone. Previous studies have shown a good correlation between the net lymphoid uptake and plasma viremia in chronic and acute infection in asymptomatic HIV-infected patients with long-term nonprogression and stable viremia [23].

Our study found that TLG and SUL metrics were high in HIV-infected patients with lymphoma irrespective of viral load. HIV-infected patients without viremia or those on ART with suppressed viral load typically demonstrate minimal or absent FDG lymph nodal uptake as opposed to patients with viremia [24]. Studies have shown a positive linear relationship between viral load and SUV of the whole-body lymphoid tissue in HIV-infected patients. A more variable relationship is seen between viral loads when regions of interest are manually drawn to obtain total lymph node SUV [25].

While quantitative FDG PET was more accurate in differentiating lymphoma from reactive lymphadenopathy in HIV-infected patients, the diagnostic accuracy appeared greater in aviremic patients. We also found that splenic SUL was higher in lymphoma than in reactive adenopathy. Only occasionally was mildly increased splenic uptake seen with high viremia in

HIV-infected patients with reactive adenopathy. This is similar to the findings of previous studies [26]. Controlling viremia prior to PET imaging by reimaging after initiation of ART when viremia is suppressed to <200 copies/mL may potentially aid interpretation of indeterminate findings in patients in whom the pattern of FDG uptake is not helpful. Practically, targeted biopsy of a hypermetabolic area would likely be performed in patients in whom malignancy is strongly suspected, rather than delay the diagnosis of lymphoma while ART therapy is being performed.

Goshen et al. similarly showed a high sensitivity of PET/CT in diagnosing lymphoma in seven HIV-infected patients with known non-Hodgkin lymphoma and one patient with suspected lymphoma and palpable lymphadenopathy, although their results showed a high false-positive rate (25 %) [27]. They suggested that in patients with normal-sized nodes with discordant CT findings, correlation with CD4 and viral load may support a benign diagnosis and avoid further investigations. This view is supported by our data. However, the false-positive rate in our study was much lower, which may have been due to accounting for both the pattern and quantitative extent of metabolic uptake. Our data concur with the findings of previous studies showing that the degree of FDG uptake is related to viral load in reactive adenopathy [3, 28], and we demonstrated a significant correlation between viral load and SUL uptake in HIV-infected patients with reactive adenopathy. This differs from the findings of Brust et al. [25], which may have been due to differences in the patient populations, levels of viremia and SUL-Max threshold. We also found lower metabolic uptake in aviremic HIV-infected patients with reactive adenopathy [25].

Qualitative scoring is a typical method used for scoring PET images. Using our scoring system, the qualitatively hottest node did not allow differentiation of lymphoma from reactive adenopathy. Quantitative PET metrics performed significantly better than qualitative visual scores in our population, although qualitative symmetry assessment was valuable.

A possible potential limitation of our study was that our population of HIV-infected patients with lymphoma had relatively advanced disease (stage III or IV disease in 16 of 19 patients). Most lymphomas in HIV-infected patients are typically high-grade large-cell, immunoblastic type with extranodal involvement common. Our patients were likely quite representative of the HIV-positive NHL patient population. Another potential limitation of our study was that we used a low-dose CT protocol without contrast enhancement which may have been of suboptimal diagnostic quality for analyzing CT nodal size. This may have biased the study results in favor of PET.

It is encouraging that the PERCIST-derived SUL-Peak uptake and TLG were quite accurate for diagnostic purposes, but they did not perform any better than the simple SUL-Max value. Due to stability of liver SUL, we used a TLG threshold

based on the mean liver SUL [29]. TLG and SUL-Peak performed comparably in our patients (Tables 2 and 3). Another potential limitation of our study was the retrospective design. However, our patients were undergoing clinical PET/CT studies in relevant clinical situations. Patients with reactive adenopathy were considered to possibly have lymphoma or infection in their differential diagnosis and showed similar CT nodal size compared to the patients with lymphoma. A prospective study using the quantitative techniques described to validate their clinical significance in a larger patient population is warranted.

Conclusion

Quantitative PET metabolic metrics as well as the qualitative assessment of symmetry of nodal uptake appear to be valuable tools for differentiating lymphoma from reactive adenopathy in HIV-infected patients using FDG PET. These parameters appear more robust in aviremic patients.

Acknowledgments We thank Dr. Richard Ambinder for his contribution, which included experimental design and thoughts on clinical relevance. We also thank Judy Buchannan for helping edit and improve the manuscript. The work was supported by a Quantitative Imaging Network grant awarded by the National Cancer Institute (NCI-U-01-CA 140204).

Conflicts of interest None.

References

1. Moir S, Chun TW, Fauci AS. Pathogenic mechanisms of HIV disease. *Annu Rev Pathol.* 2011;6:223–48.
2. Beral V, Peterman T, Berkelman R, Jaffe H. AIDS-associated non-Hodgkin lymphoma. *Lancet.* 1991;337:805–9.
3. Bower M, Palmieri C, Dhillon T. AIDS-related malignancies: changing epidemiology and the impact of highly active antiretroviral therapy. *Curr Opin Infect Dis.* 2006;19:14–9.
4. Shiels MS, Pfeiffer RM, Gail MH, Hall HI, Li J, Chaturvedi AK, et al. Cancer burden in the HIV-infected population in the United States. *J Natl Cancer Inst.* 2011;103:753–62.
5. Scharko AM, Perlman SB, Pyzalski RW, Graziano FM, Sosman J, Pauza CD. Whole-body positron emission tomography in patients with HIV-1 infection. *Lancet.* 2003;362:959–61.
6. Liu Y. Demonstrations of AIDS-associated malignancies and infections at FDG PET-CT. *Ann Nucl Med.* 2011;25:536–46.
7. Love C, Tomas MB, Tronco GG, Palestro CJ. FDG PET of infection and inflammation. *Radiographics.* 2005;25:1357–68.
8. Keidar Z, Gurman-Balbir A, Gaitini D, Israel O. Fever of unknown origin: the role of 18F-FDG PET/CT. *J Nucl Med.* 2008;49:1980–5.
9. Kouijzer IJ, Bleeker-Rovers CP, Oyen WJ. FDG-PET in fever of unknown origin. *Semin Nucl Med.* 2013;43:333–9.
10. Bental M, Deutsch C. Metabolic changes in activated T cells: an NMR study of human peripheral blood lymphocytes. *Magn Reson Med.* 1993;29:317–26.
11. Haase AT, Henry K, Zupancic M, Sedgewick G, Faust RA, Melroe H, et al. Quantitative image analysis of HIV-1 infection in lymphoid tissue. *Science.* 1996;274:985–9.

12. Juweid ME, Stroobants S, Hoekstra OS, Mottaghy FM, Dietlein M, Guermazi A, et al. Use of positron emission tomography for response assessment of lymphoma: consensus of the Imaging Subcommittee of International Harmonization Project in Lymphoma. *J Clin Oncol*. 2007;25:571–8.
13. O'Doherty MJ, Barrington SF, Campbell M, Lowe J, Bradbeer CS. PET scanning and the human immunodeficiency virus-positive patient. *J Nucl Med*. 1997;38:1575–83.
14. Goudarzi B, Jacene HA, Wahl RL. Measuring the “unmeasurable”: assessment of bone marrow response to therapy using FDG-PET in patients with lymphoma. *Acad Radiol*. 2010;17(9):1175–85.
15. Lodge MA, Chaudhry MA, Udall DN, Wahl RL. Characterization of a perirectal artifact in 18F-FDG PET/CT. *J Nucl Med*. 2010;51(10):1501–6.
16. Liu Y. Concurrent FDG avid nasopharyngeal lesion and generalized lymphadenopathy on PET-CT imaging is indicative of lymphoma in patients with HIV infection. *AIDS Res Treat*. 2012; 2012:764291.
17. Wahl RL, Jacene H, Kasamon Y, Lodge MA. From RECIST to PERCIST: evolving considerations for PET response criteria in solid tumors. *J Nucl Med*. 2009;50 Suppl 1:122S–50.
18. Frisch M, Biggar RJ, Engels EA, Goedert JJ, AIDS-Cancer Match Registry Study Group. Association of cancer with AIDS-related immunosuppression in adults. *JAMA*. 2001;285:1736–45.
19. Aldous JL, Haubrich RH. Defining treatment failure in resource-rich settings. *Curr Opin HIV AIDS*. 2009;4:459–66.
20. Landis JR, Koch GG. The measurement of observer agreement for categorical data. *Biometrics*. 1977;33:159–74.
21. Scadden DT. AIDS-related malignancies. *Annu Rev Med*. 2003;54:285–303.
22. Song MK, Chung JS, Shin HJ, Moon JH, Lee JO, Lee HS, et al. Prognostic value of metabolic tumor volume on PET/CT in primary gastrointestinal diffuse large B cell lymphoma. *Cancer Sci*. 2012;103:477–82.
23. Iyengar S, Chin B, Margolick JB, Sabundayo BP, Schwartz DH. Anatomical loci of HIV-associated immune activation and association with viraemia. *Lancet*. 2003;362:945–50.
24. Lim ST, Karim R, Nathwani BN, Tulpule A, Espina B, Levine AM. AIDS-related Burkitt's lymphoma versus diffuse large-cell lymphoma in the pre-highly active antiretroviral therapy (HAART) and HAART eras: significant differences in survival with standard chemotherapy. *J Clin Oncol*. 2005;23:4430–8.
25. Brust D, Polis M, Davey R, Hahn B, Bacharach S, Whatley M, et al. Fluorodeoxyglucose imaging in healthy subjects with HIV infection: impact of disease stage and therapy on pattern of nodal activation. *AIDS*. 2006;20:985–93.
26. Mbulaiteye SM, Parkin DM, Rabkin CS. Epidemiology of AIDS-related malignancies an international perspective. *Hematol Oncol Clin North Am*. 2003;17:673–96.
27. Goshen E, Davidson T, Avigdor A, Zwas TS, Levy I. PET/CT in the evaluation of lymphoma in patients with HIV-1 with suppressed viral loads. *Clin Nucl Med*. 2008;33:610–4.
28. Lucignani G, Orunesu E, Cesari M, Marzo K, Pacei M, Bechi G, et al. FDG-PET imaging in HIV-infected subjects: relation with therapy and immunovirological variables. *Eur J Nucl Med Mol Imaging*. 2009;36:640–7.
29. Paquet N, Albert A, Foidart J, Hustinx R. Within-patient variability of (18)F-FDG: standardized uptake values in normal tissues. *J Nucl Med*. 2004;45:784–8.